Exotic Searches with ATLAS

E. Kay
CERN, Espl. des Particules 1, 1211 Meyrin
on behalf of the ATLAS Collaboration[a]

In these proceedings, recent highlights of searches for exotic new physics using the ATLAS detector at the LHC are presented.

ATL-PHYS-PROC-2024-034
14 May 2024

1 Introduction

Despite the tremendous success of the Standard Model (SM) in describing the majority of our observations in particle physics thus far, many gaps in our understanding of nature remain, motivating us to seek solutions beyond the Standard Model (BSM). With the wide variety of outstanding physics questions, concerning topics from the hierarchy problem to matter-antimatter asymmetry and the origin of dark matter, the hunt for BSM physics involves a comprehensive collection of analyses spanning many theories and kinematic ranges. The ATLAS experiment [1], situated at one of the collision points of the Large Hadron Collider (LHC) at CERN, employs an appropriately diverse physics programme. In these proceedings, recent searches for leptoquarks, new heavy gauge bosons and heavy scalars using the full Run 2 data sample, corresponding to an integrated luminosity of 139 fb^{-1} recorded by ATLAS between 2015 and 2018 are presented.

2 Leptoquark Searches

Leptoquarks (LQ) are hypothetical particles which carry both baryon and lepton quantum numbers. They are either scalar (spin zero) or vector (spin one) particles, carry colour and have a fractional electric charge. They therefore couple simultaneously to both quarks and leptons, providing a connection between the lepton and quark sectors. LQs have been postulated in the context of a broad range of theories, such as unified, technicolour and composite models. In the past decade, there has been renewed interest in LQs due to their potential connection to anomalies in various measurements of B-meson decays. While a recent reanalysis of data from the LHCb Collaboration has yielded results in agreement with lepton-flavour universality [?], other

Table 1: Summary of the searches involved in the third generation LQ combination (for which references can be found in [4]). For each final state, the LQ scenarios relevant to this channel are indicated with a tick. Adapted from Ref. [4].

	Scalar				Vector		Signal Region		
Final State	LQ_3^u	LQ_3^d	LQ_{mix}^u	LQ_{mix}^d	$U_1^{\text{YM/MC}}$	$\widetilde{U}_1^{\text{YM/MC}}$	N_ℓ	$N_{\tau_{\text{had.}}}$	$N_{\text{b-jet}}$
$t\nu b\tau$	✓	✓	-	-	✓	-	0	1	$\geqslant 2$
$b\tau b\tau$	✓	-	-	-	✓	-	$\{0,1\}$	$\{1,2\}$	$\{1,2\}$
$t\tau t\tau$	-	✓	-	-	-	✓	$\{1,2,3\}$	$\geqslant 1$	$\geqslant 1$
$t\nu b\ell$	-	-	✓	✓	-	-	1	-	$\geqslant 1$
$b\ell b\ell$	-	-	✓	-	-	-	2	-	$\{0,1,2\}$
$t\ell t\ell$ (2ℓ)	-	-	-	✓	-	-	2	-	
$t\ell t\ell$ $(\geqslant 3\ell)$	-	-	-	✓	-	-	$\{3,4\}$	-	$\geqslant 2$
$t\nu t\nu$	✓	-	✓	-	✓	-	0	0	$\geqslant 2$
$b\nu b\nu$	-	✓	-	✓	-	-	0	-	$\geqslant 2$

anomalies, such as those in the $b \to s\mu\mu$ angular distribution or in charged-current $b \to c\ell\mu$ transitions, remain [3].

Leptoquarks may be produced at the LHC either singly or in pairs. Both cases are covered in the wide range of ATLAS LQ searches, so as to increase our reach for discovery through their complementarity. Single LQ production is more relevant for large $LQ - q - \ell$ Yukawa-style couplings (λ) or large LQ mass (m_{LQ}). In the case of pair production, which would proceed mainly via gluon–gluon fusion or quark–antiquark annihilation, there is less dependence on λ, and one can target lower values of this coupling.

A recent result published by ATLAS [4] focuses on pair-produced LQs which preferentially decay to third-generation quarks. It is, in fact, a combination of nine independent searches which are sensitive to different LQ decay modes. As summarised in Table 1, the searches target final states with light leptons (e/μ), hadronically decaying taus (τ), jets, b-jets and missing transverse energy ($E_{\text{T}}^{\text{miss}}$) in the final state, but with differing selection criteria. Great care is taken to ensure that all participating signal regions are orthogonal, with overlap removal performed where necessary. The third-generation scalar LQs considered here may be of up-type (u) or down-type (d), with charges of $\pm\frac{2}{3}$ and $\pm\frac{1}{3}$, respectively, and may undergo same generation (LQ_3) or mixed generational (LQ_{mix}) decays. Two vector models, U_1 and $\widetilde{U}_1$, are considered, where the latter carries a charge of $\pm\frac{5}{3}$, meaning only the $t\tau t\tau$ channel is eligible for this interpretation. For vector LQs, the pair-production cross-section depends not only on m_{LQ}, but also on the coupling to gluons. An additional coupling of Yang–Mills (YM) type is varied, leading to two coupling scenarios for each considered vector model: YM or 'minimal coupling' (MC).

In the case of scalar LQs, the eligible analyses are combined to produce two-dimensional exclusion limits as a function of m_{LQ} and the branching fraction ($\mathcal{B}$) to the relevant final state. The left-hand plot of Figure 1 gives an example, in this case for the LQ_3^u scenario. Limits obtained through the individual analyses are compared here, and their complementarity is illustrated by their contrasting coverage of the $\mathcal{B}$ parameter space. When these results are combined, the limit is improved by up to 100 GeV for intermediate values of $\mathcal{B}$. This level of improvement is seen across the considered scalar LQ scenarios for this search.

Limits on the production cross-section of U_1-vector LQs as a function of mass are also produced, assuming a branching fraction of 0.5. An example is shown in the right-hand plot of Figure 1, in this case for the MC scenario. Once again, limits obtained through the individual analyses are overlaid with the combined result, and in this case the combination of the three eligible analyses yields an improvement on the lower mass limits of around 70 GeV.

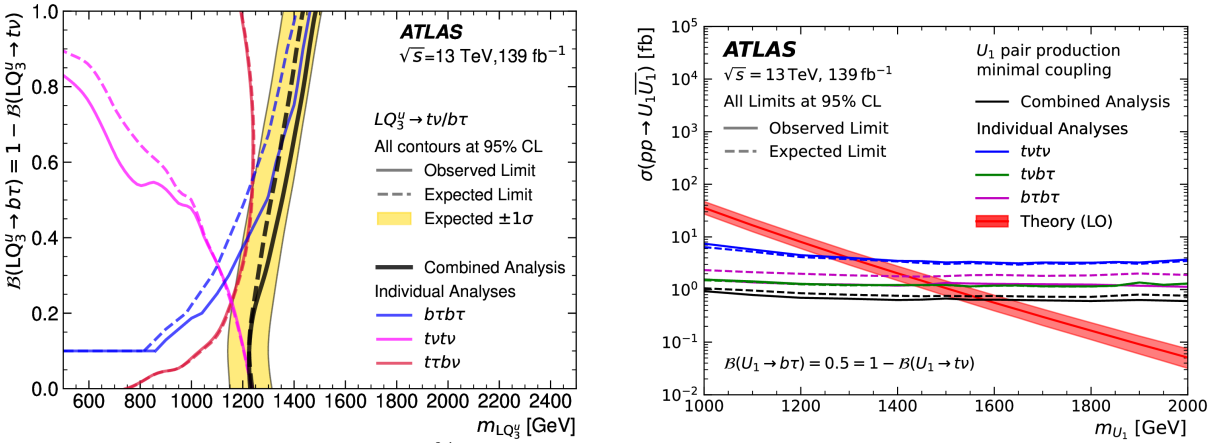

Figure 1: Expected and observed 95% CL exclusion limits for two of the considered LQ models. The left-hand plot shows limits for up-type scalar LQs decaying into a third-generation quark and lepton, presented in terms of the LQ mass and the branching fraction to a charged lepton. The right-hand plot shows limits on the U_1^{MC} production cross-section as a function of the LQ mass, assuming a branching fraction to a τ-lepton of 0.5. In both cases, coloured lines indicate the limits set by individual analyses, while the combined limits are marked with black lines. Both plots are taken from Ref. [4].

3 Heavy Gauge Boson Searches

New heavy gauge bosons are predicted in a plethora of extensions of the SM. The LHC allows us to probe increasingly higher masses in pursuit of such particles and, as a result, many searches for them have been undertaken by ATLAS, setting lower mass limits as high as 6 TeV [5]. Many such searches have been conducted in the context of simplified benchmark models, such as the Sequential Standard Model (SSM) [6] and Heavy Vector Triplet (HVT) model [7] [8].

A recent example of such an analysis targets W' bosons decaying to a τ-lepton and a neutrino [11]. This analysis can complement similar searches involving light leptons when considering flavour-universal models, such as the SSM, where the W' and Z' couplings to fermions are identical to those of their SM counterparts. Additionally, this search considers non-universal gauge interaction models (NUGIM), where couplings can differ between the three lepton generations. In NUGIM scenarios, the non-universality of the W' couplings to the SM fermions is parametrised by an angular parameter, θ_{NU}.

The decay products from the W' decay are expected to be back-to-back in the transverse plane, with the neutrino from the subsequent decay of the τ-lepton partially cancelling the $E_{\mathrm{T}}^{\mathrm{miss}}$ arising from the prompt neutrino. The variable used to discriminate between signal and background is the transverse mass (m_T), which is constructed using the $E_{\mathrm{T}}^{\mathrm{miss}}$, the transverse momentum of the visible τ decay products and the azimuthal angle between these two.

Limits on the cross-section and branching fraction as a function of resonance mass in the context of the SSM are shown in the left-hand plot of Figure 2. Here, W' masses up to 5 TeV are excluded, greatly improving upon early Run 2 results for the same channel (which are overlaid on the same plot). Limits on the resonance mass and mixing angle θ_{NU} in the context of the NUGIM model are shown in the right-hand plot of Figure 2: here, the blue shaded area is excluded by this analysis, and can be compared to the equivalent Run 2 light lepton search as well as previous iterations of the τ-channel analyses. Aside from the huge gain in statistics between the partial and full Run 2 datasets used in this and the previous iteration, these stronger limits can be owed to improved analysis techniques, as well as advances in τ identification and reconstruction.

As already evidenced by the aforementioned LQ search, combining our analyses can make the most of our results and help us to explore the maximum extent of the targeted parameter space for our chosen models. In this spirit, a recent combination [10] of eighteen published di-quark, di-lepton and di-boson heavy resonance searches (including the one which was just discussed)

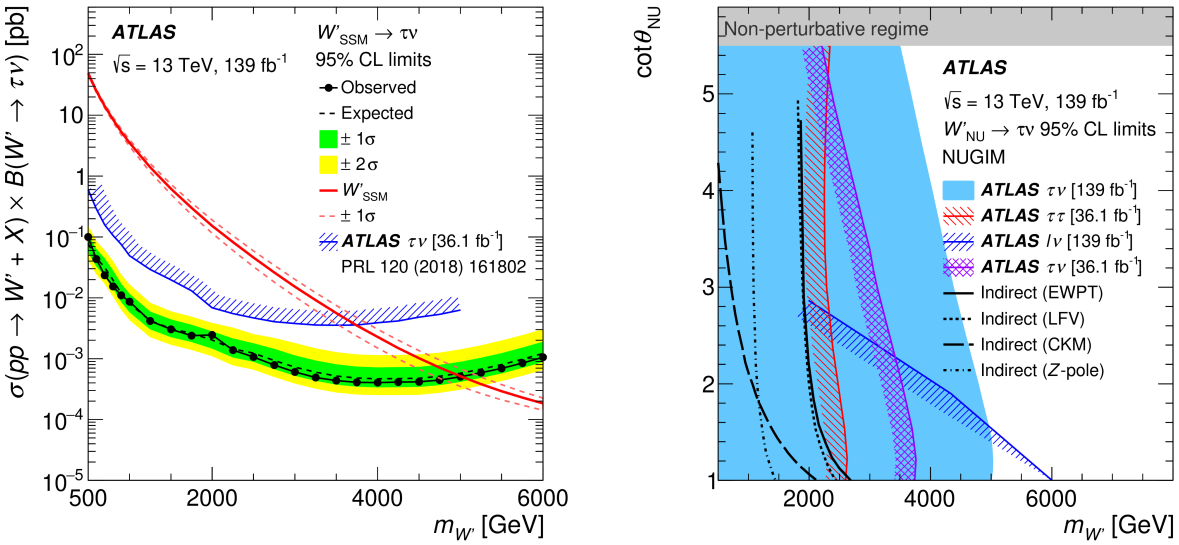

Figure 2: The left-hand plot shows observed (black markers) and expected (black dashed line) 95% CL upper limits on the cross-section times branching ratio ($\sigma \times B$) as a function of the W' resonance mass in the context of the SSM, with a blue hatched line indicating the limits obtained from a previous iteration of this analysis [9]. The right-hand plot shows limits on the resonance mass as a function of the $\cot\theta_{\mathrm{NU}}$ in the context of a NUGIM model, where the blue shaded area represents the exclusion limits set by the described analysis, while other lines indicate results from other ATLAS W' searches or overlaid data from various measurements. Both plots from Ref. [11].

was undertaken. As with other such efforts, the individual results are validated, and many checks are performed to ensure orthogonality between them, both in terms of event overlaps and also definitions of objects and systematic uncertainties. The combination is performed in the context of an HVT framework, which gives rise to a set of nearly degenerate charged W' and neutral Z' states, collectively referred to as V', and allows for the exploration of different coupling strengths of those states to quarks (g_q), leptons (g_ℓ), vector bosons (g_V), and Higgs bosons (g_H).

A step-by-step approach to combination is employed in this search, meaning that various sub-combinations and comparisons of sub-sets of the considered analyses are scrutinised before performing a full combination of all results. The left-hand plot of Figure 3 shows an exclusion contour on couplings to third-generation quarks and leptons, where the previously described $W' \to \tau\nu$ analysis contributes to constraining the lepton coupling. An example of results from the full combination is shown in the right-hand plot of Figure 3, this time in terms of Higgs and fermion couplings (g_f), where all but a narrow region of g_f is excluded by the combined results.

4 Searches for Heavy Scalars

New massive (pseudo-)scalar states with strong couplings to top quarks are also predicted in numerous BSM models, such as Two-Higgs-Doublet Models (2HDMs), which introduce five physical states: a light CP-even boson (h), a heavier CP-even boson (H), a CP-odd boson (A) and two charged bosons ($H^{+/-}$). Many searches target such models and cover a considerable range of scalar masses ($m_{A/H}$) and $\tan\beta$, i.e. the ratio of vacuum expectation values for the doublets [12]. There is a notable gap in this coverage for high $m_{A/H}$ and low $\tan\beta$, therefore this region of the parameter space has been of particular interest.

For type-II 2HDMs, such as the Minimal Supersymmetric SM (MSSM), $A/H \to t\bar{t}$ is the dominant decay mode for small $\tan\beta$. A recent full Run 2 ATLAS analysis targeting this channel [13] is described elsewhere in these conference proceedings. While the relatively high production cross-section for this process is an attractive prospect, complications arise due to interference between the irreducible $gg \to t\bar{t}$ SM background and top-quark loops which appear in the dom-

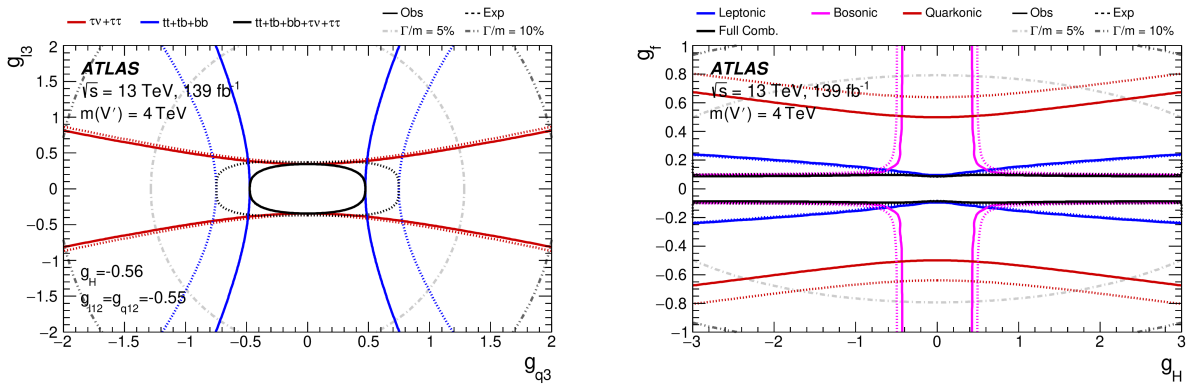

Figure 3: 95% CL observed and expected upper limit contours in 2D coupling planes for various sub-combinations considered, assuming a signal pole mass of 4 TeV. The left-hand plot presents the $\{g_{q3}, g_{\ell 3}\}$ plane, while the $\{g_H, g_f\}$ plane is shown in the right-hand plot. In both cases, coloured lines indicate exclusions set by sub-combinations of results which are sensitive to the presented coupling. Combinations of all contributing analyses for each plot are shown in black. Both taken from Ref. [10].

inant gluon-gluon fusion production mode for this channel. Though associated production of H/A with $t\bar{t}$ is a sub-dominant production mode, it is far less susceptible to this interference.

The latest ATLAS search for $pp \to t\bar{t}H/A \to t\bar{t}$ [14] focuses on 1-lepton (1L) and 2-opposite-sign-lepton (2LOS) final states. Events feature high jet and b-jet multiplicities, and the dominant backgrounds are $t\bar{t}$+jets and SM 4-top production. Known issues affect the modelling of the $t\bar{t}$+jets background from simulations, impacting the kinematics in the high jet multiplicity regime and the cross-section of $t\bar{t}$+heavy-flavour production. This analysis therefore adopts data-driven methods in order to correct for these effects. Events passing a preselection are categorised into orthogonal regions, some of which are used to derive these data-driven corrections, while others are used as control (CR) and signal regions (SR) for setting limits on the signal. The left-hand plot of Figure 4 compares the transverse momentum sum of reconstructed leptons and jets (H_T) before and after this correction for a 2LOS region, with a clear improvement of the modelling visible in the ratio plot (lower part of the figure). In the SRs, a multivariate analysis based on $m_{A/H}$-parametrised graph neural networks (GNNs) is performed in order to optimise the separation between signals and backgrounds.

In the absence of any significant excess over the SM prediction, limits are set on the heavy scalar mass. Limits from this analysis are combined with those from a previous search in the two-lepton-same-sign / multi-lepton (2LSS/ML) [15], with results presented in terms of $\tan\beta$ for a scenario where $m_H = m_A$, as shown in the right-hand plot of Figure 4.

5 Conclusions

ATLAS has a diverse BSM search programme, with many new results published and in progress for the full LHC Run 2 dataset. Only a handful of the latest results were presented here, and many others are covered during this conference. Though these analyses unfortunately did not uncover new physics, great improvements were made upon previous results through the use of advanced analysis techniques and by performing statistical combinations. Run 3 of the LHC is ongoing, with 13.6 TeV collision energy and the inclusion of multiple upgrades [16], providing exciting prospects for new and improved searches with this new dataset.

References

1. ATLAS Collaboration, JINST **3**, S08003 (2008).
2. LHCb Collaboration, *Phys. Rev.* D **108**, 032002 (2023).
3. A. Crivellin, arXiv:2304.01694 [hep-ph].

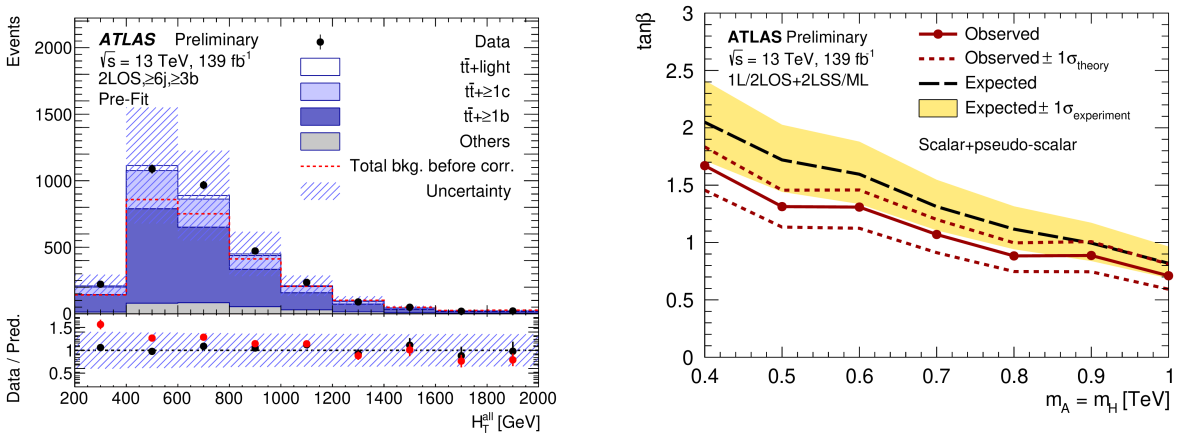

Figure 4: The left-hand plot shows a comparison of the H_T distributions between data and prediction before (red) and after (black) applying data-driven corrections for a 2LOS region. The right-hand plot shows expected and observed 95% CL lower limits on $\tan\beta$ as a function of the (pseudo-)scalar mass obtained through a combination of the 1L/2LOS analysis described here and the 2LSS/ML analysis. In this case, both scalar and pseudo-scalar states contribute, with $m_H = m_A$. Both plots are taken from Ref. [14].

4. ATLAS Collaboration, CERN-EP-2023-288, arXiv:2401.11928 [hep-ex].
5. ATLAS Collaboration, ATL-PHYS-PUB-2023-008, https://cds.cern.ch/record/2853754.
6. Cheng-Wei Chiang et al., *Phys. Rev.* D **85** (2012).
7. Duccio Pappadopulo et al., JHEP **2014** (2014).
8. Michael J. Baker et al., JHEP **2022** (2022).
9. ATLAS Collaboration, *Phys. Rev.* D **120**, 161802 (2018).
10. ATLAS Collaboration, CERN-EP-2024-039, arXiv:2402.10607 [hep-ex].
11. ATLAS Collaboration, CERN-EP-2023-298, arXiv:2402.16576 [hep-ex].
12. ATLAS Collaboration, ATL-PHYS-PUB-2022-043, https://cds.cern.ch/record/2827098.
13. ATLAS Collaboration, ATLAS-CONF-2024-001, https://cds.cern.ch/record/2891813.
14. ATLAS Collaboration, ATLAS-CONF-2024-002, https://cds.cern.ch/record/2891814.
15. ATLAS Collaboration, JHEP **07**, 203 (2023).
16. ATLAS Collaboration, CERN-EP-2022-259, arXiv:2305.16623 [physics.ins-det].